Formation of Hierarchical 2D-Mos_2 Nanostructures over Carbon Fabric as Binder Free Electrode Material for Supercapacitor Applications

Selvaraj Shanthi[1,2,3], Yasuhiro Hayakawa[2], Suru Ponnusamy[3], Hiroya Ikeda[2]** and Chellamuthu Muthamizhchelvan[3]*

[1]Graduate School of Science and Technology, Shizuoka University, Japan

[2]Research Institute of Electronics, Shizuoka University, Japan

[3]Department of Nanotechnology, SRM Institute of Science and Technology, India

shanthiselvaraj43@gmail.com, hayakawa.yasuhiro@shizuoka.ac.jp, suruponnus@gmail.com, **ikeda.hiroya@shizuoka.ac.jp, *selvancm@gmail.com

Abstract

Carbon fabrics are the new generation promising electrode materials for super capacitors owing to their high electrical conductivity, high chemical stability and low thermal expansion. In this work, 2D-MoS_2 nanostructures have been successfully deposited over the commercially available carbon fabric by hydrothermal approach, using silicontungstic acid as an additive. MoS_2 nanostructures – carbon fabric was broadly characterized using XRD, FESEM and Raman Spectroscopy. XRD patterns indicated that the fabricated MoS_2 nanoparticles can be indexed to hexagonal (2H) and rhombohedral (3R) phases. FESEM images revealed the formation of hierarchical 2D MoS_2 nanosheets arranged in a nanosphere like morphology over the carbon fabric. The electrochemical behavior of the MoS_2 - carbon fabric and commercially available bare carbon fabric were studied using cyclic voltammetry analysis with different scan rates. The MoS_2-carbon fabric exhibited an excellent electrochemical performance with a specific capacitance of 441 F/g at a scan rate of 10mV/s. The good cyclic behavior with symmetric charging/discharging curves, constant specific capacitance for longer scan rates, suggesting that the MoS_2- carbon fabric electrode is a potential electrode material for high power applications.

Keywords: Carbon Fabrics (CF); 2D materials; MoS_2 Nanosheets; binder-free electrode; Supercapacitors;

Introduction

Supercapacitors, also known as electrochemical capacitors, have been acknowledged for over fifty years and considered as one of the potential energy storage systems in addition to batteries, for various diverse applications such as portable electronics, surge power delivery devices for electric vehicles and digital calipers [1]. In recent years, tremendous efforts have been made to develop the electrode materials for supercapacitor applications to meet the energy requirements of daily life. The electrode materials for supercapacitor falls under three categories namely electrical double layer capacitors (EDLC), pseudocapacitors and hybrid capacitors [2-7]. In EDLC, the electrical energy can be stored based on the following phenomena of either charge accumulation at the electrode and electrolyte interface, e.g., carbon-based materials and graphene, which has high surface area, excellent electrical conductivity. In pseudocapacitors, the energy can be stored by reversible faradic redox reactions, e.g., transition metal oxides/hydroxides and conducting polymers, which has high specific capacitance and energy density. The hybrid capacitors are the combination of EDLC and pseudocapacitors.

Scientific community people are focusing on fabricating the high-performance supercapacitor with excellent electrochemical performance, flexible, binder free to their potential applications in flexible energy storage devices. To achieve the high-performance supercapacitors, hybrid electrode materials are highly recommended because of having excellent electrical conductivity, high surface area and high theoretical capacitance values. Recently, two-dimensional (2D) materials like transition metal dichalcogenide (TMD) such

as MoS_2, WS_2, and SnS_2 have gained attraction because of their unique electrical, optical and mechanical properties [8].

Among these, 2D-TMD materials MoS_2 has attained special attention because of its earth abundant, large surface area and 2D structure preferring ion adsorption and transports but limited by its low intrinsic conductivity which leads to low energy density [9,10]. Additionally, while preparing the MoS_2 based electrode materials, utilizing the binders and conductive agents decreases the energy density [11]. By considering the above facts, binder free fabrication of MoS_2 nanostructures over the conductive substrates are quite appealing to develop the supercapacitors with excellent electrochemical performance. Because of inimitable properties like high flexibility, low cost, excellent electrical conductivity, good physical strength, carbon fabric (CF) is highly recommended to fabricate the binder-free electrodes for supercapacitor applications [12].

In this work, we report the simple hydrothermal synthesis of agglomerated 2D MoS_2 nanosheets arranged over the commercially available CF, like 2D MoS_2 nanospheres morphology. The electrochemical performances of the fabricated MoS_2 – CF was further investigated using electrochemical measurement system. It was found that the supercapacitor constructed with this type of binder-free electrode material exhibited a specific capacitance of 441 F/g at the scan rate of 10mV/s, which offers a new generation two-dimensional electrode material for supercapacitors. For comparison, the electrochemical investigation of commercially available CF was also performed to check the influence of 2D MoS_2 for the supercapacitor applications.

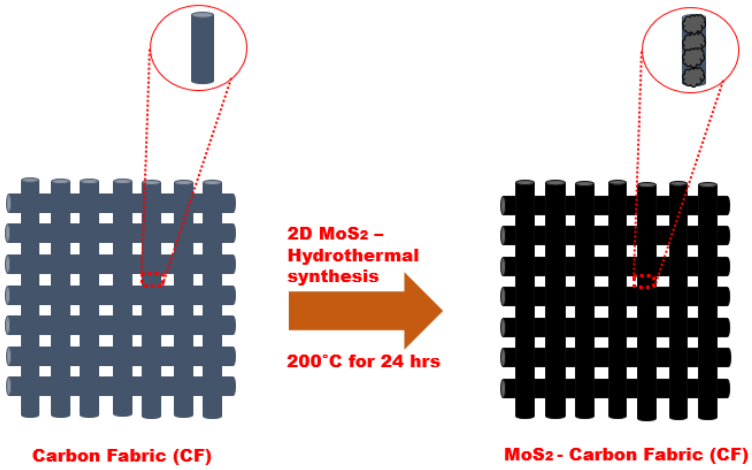

Fig.1. Schematic representation- Fabrication of MoS_2 nanostructures over CF, using hydrothermal synthesis.

Materials and Methods

All chemicals used were of analytical grade, purchased from Wako chemicals, Japan. Carbon fabric (CF) was purchased from sainergy fuel cell India, pvt limited. The commercially available bare CF and the fabricated binder free 2D-MoS_2-CF electrodes were studied using X-ray diffractometer, XRD (RINT-2200, CuKα radiation, Rigaku) with 0.04 °sec-1 scan rate in the 2θ range from 20° to 80°, Raman scattering spectroscopy (NRS-7100, JASCO) with a laser excitation wavelength of 532 nm (spot size 1 μm) and field-emission scanning electron microscopy, FE-SEM (JSM 6335F, JEOL). Electrochemical characterizations were performed using CHI 600 series standard three electrode electrochemical Analyzer/Workstation. Here, the MoS_2 – CF as working electrode, Ag/AgCl (saturated KCl) as reference electrode and platinum wire as counter electrode were used along with 0.5M of Con.H_2SO_4 as an electrolyte, during the electrochemical analysis. Electrochemical impedance spectroscopy (EIS) analysis were also carried out from 100 kHz (Higher frequency) to 0.1 Hz (lower frequency) at open circuit potential with an AC perturbation voltage of about 5 mV.

Figure 1 shows the schematic representation of fabrication of MoS_2 nanostructures over CF, using hydrothermal synthesis. Prior to synthesis, commercially available CF was treated in ultrasonic bath with

ethanol for about 1 hour, and then washed with distilled water to remove the impurities, which was used as a conductive template for the growth of MoS_2 nanostructures. 0.5 g of Na_2MoO_4 .$2H_2O$ and 0.7g of CH_3CSNH_2 were dissolved in 50ml of distilled water. Then, 8.0g of sillicontungstic acid was added into the reaction mixture solution under vigorous stirring. The mixture solution along with the CF was then transferred into a 100 mL Teflon-lined stainless-steel autoclave apparatus and kept at 200 °C for 24 hrs. After cooling to room temperature, the fabricated binder free MoS_2 – CF electrode was taken from the autoclave and washed with absolute ethanol and distilled water for several times and annealing at 300 °C for 5 hrs.

The capacitance values were calculated from CV data according to the following equation,

$$C_{device} = \frac{1}{v(V_f - V_i)} \int_{Vi}^{Vf} I(V)dV \quad \text{..... (Equation 1)}$$

where v is the scan rate, V_f and V_i are integrated potential limits of voltammetric curve and I(V) is the voltammetric discharge current. Specific capacitance of the electrodes can be calculated by the relation,

$$C = \frac{C_{device}}{m} \quad \text{.....(Equation 2)}$$

Where, m is the mass of the electrode material, respectively.

Results and Discussion

For the growth mechanism [13], it is clearly characterized that the chemical reaction of sodium molybdate with sillicontungstic acid tends to form molydosilic acid (from equation 3) under acid condition whose typical form is $H_4SiMo_{12}O_{40}$. On the other hand, the Mo (VI) can be easily reduced with some reductants such as H_2S in the solution [14,15]. During the hydrothermal process, the reductant is H_2S which was provided by $CS(NH_2)_2$, (from equation 4) because $CS(NH_2)_2$ can be easily decomposed in solution [16]. Thus, the oxidation–reduction reactions held during the hydrothermal process should be responsible for the formation of agglomerated MoS_2 nanosheets in to MoS_2 nanospheres like morphology over the CF (from equation 5). The intermediate product $H_4SiMo_{12}O_{40}$ could serve as a self-sacrificial template for the subsequent growth of MoS_2 nanospheres like morphology. Based on the above analysis, the reaction mechanism for the formation of MoS_2 nanostructures can be expressed as follows:

$$Na_2MoO_4 + H_4O_{40}SiW_{12} \rightarrow H_4SiMo_{12}O_{40} + 12Na_2WO_4 \text{ ..... (Equation 3)}$$

$$CH_3CSNH_2 + 2H_2O \rightarrow H_2S + CH_3COOH + NH_3 \text{ ..... (Equation 4)}$$

$$H_4SiMo_{12}O_{40} + H_2S \rightarrow 12MoS_2 + H_2SiO_3 + 3H_2SO_4 + 25H_2O \text{..... (Equation 5)}$$

Figure 2 represents the XRD analysis of (a) commercially available CF and (b) the fabricated MoS_2 - CF. The diffraction crystal planes (002) and (100), corresponded to the hexagonal primitive structure of carbon (JCPDS 89-8487) [17]. The diffraction peaks correspond to (002), (100), (101), (103), and (105) reflections, signified the nanostructured 2H-MoS_2 (JCPDS 37-1492) [18]. And the diffraction peaks which correspond to (004), (101) indicated the nanostructured 3R-MoS_2 (JCPDS 17-0744) [19].

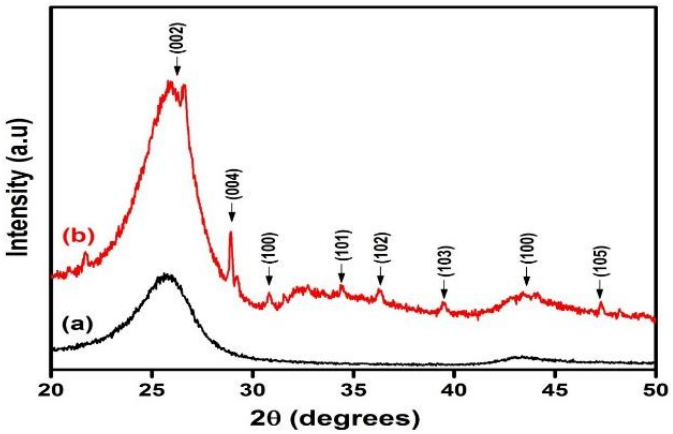

Fig. 2. XRD Analysis of (a) CF and (b) MoS_2 - CF.

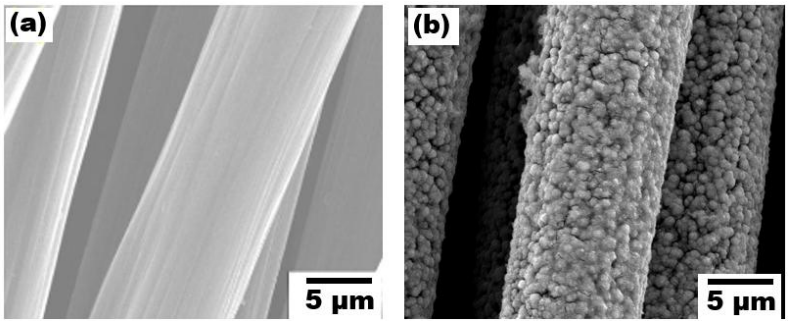

Fig.3. FESEM analysis of (a) CF and (b) MoS_2-CF.

Figure 3 shows the typical FESEM analysis of (a) CF and (b) MoS_2 – CF. From Figure 3(a), it is clearly seen that the carbon fabrics are compactly packed with random orientation in order to form a macroporous open structure [20,21]. This kind of porous material provide better accessibility to the electrolyte. Hierarchical 2D MoS_2 nanosheets were agglomerated in to MoS_2 nanosphere like morphology with uniform distribution over the CF, as shown in Figure 3(b). Thus, this type of 2D- MoS_2 nanostructures over the CF facilitates an excellent electrochemical performance for high power applications, because of its high surface area.

Figure 4 shows the Raman spectroscopy (a) CF and (b) MoS_2-CF. From the Raman spectra of Figure 4(a) and 4(b), the two high intensity peaks obtained at 1349 cm^{-1} and 1586 cm^{-1}, depicted the D and G bands of CF [22]. Hence, the calculated I_D/I_G ratio for MoS_2 – CF and CF are 1.2 and 1.14 respectively. From Figure 4(b), the obtained Raman modes (in-plane optical vibration of Mo and S atoms) E^1_{2g} (403 cm^{-1}) and E^2_{2g} (377 cm^{-1}), with the frequency difference of 26 cm^{-1}, represented the five-layer formation [23].

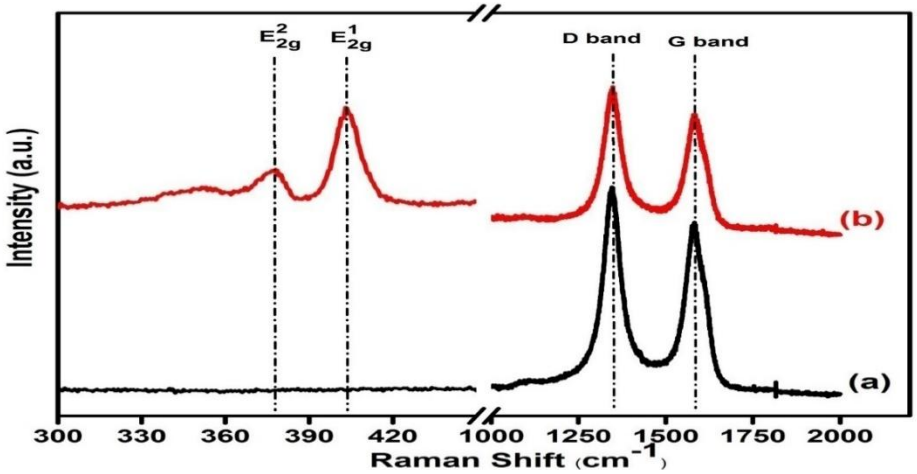

Fig. 4. Raman spectroscopy analysis of (a) CF and (b) MoS_2 – CF.

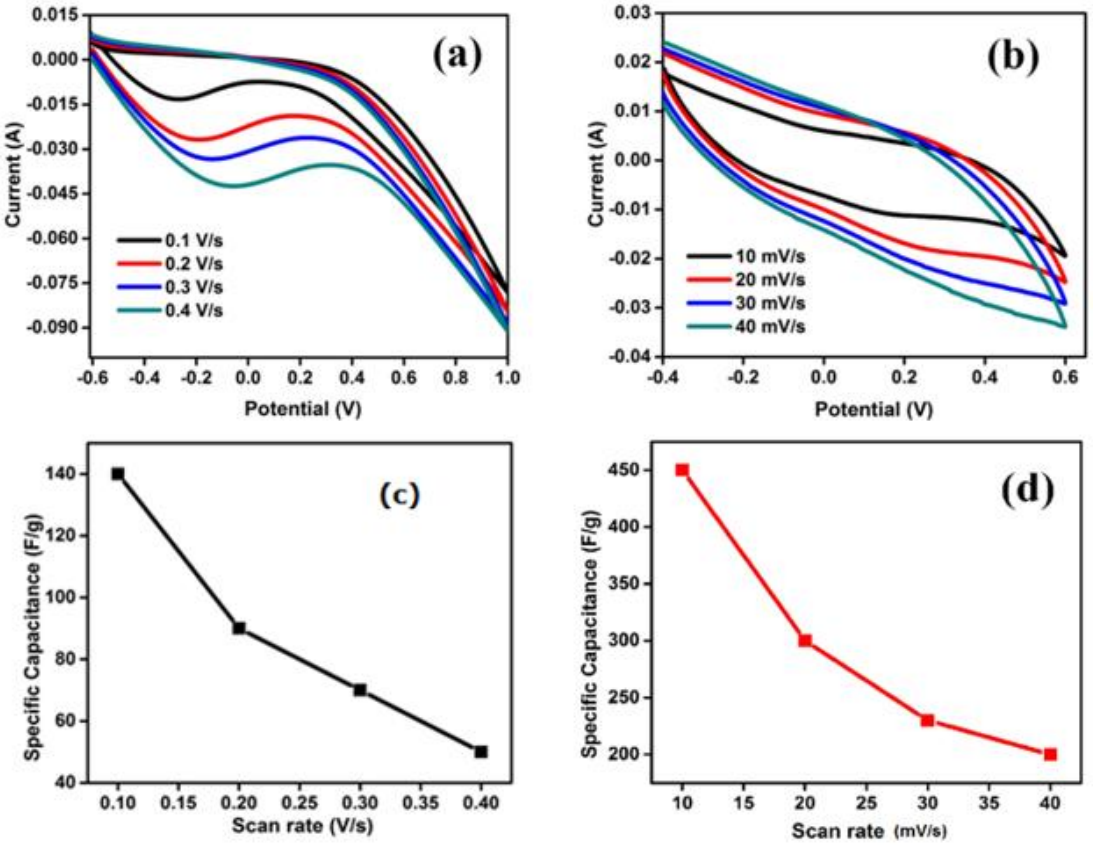

Fig. 5. Cyclic Voltammertry (CV) analysis of (a) CF and (b) MoS_2 – CF. Relation between Specific capacitance and Scan rate.

The cyclic voltammetry (CV) analysis of CF and MoS_2 – CF were shown in Figure 5(a) and (b). The CV analysis of CF exhibited an exceptional performance with asymmetric curve pattern of charging/discharging electrochemical behavior of specific capacitance value as 145F/g at the scan rate of 0.1V/s, as shown in Figure 5(a). From Figure 5(b), it is clearly seen that the fabricated binder free MoS_2 -CF exhibited an enhanced electrochemical performance with almost rectangular pattern of cyclic loop with maximum specific capacitance value as 441 F/g at the scan rate of 10mV/s. The enhancement in capacitance is due to the increased surface area of MoS_2 – CF. This behavior of symmetric in charging and discharging cycles helps to use it in high power applications. This linear and symmetric curve exposed the good capacitive electrochemical behavior of MoS_2 – CF. Variations of specific capacitance for different scan rates were represented in Figure 5(c) and (d). It revealed that constant value of specific capacitance can be achieved at higher scan rates, which is the potential significance of the electrode materials.

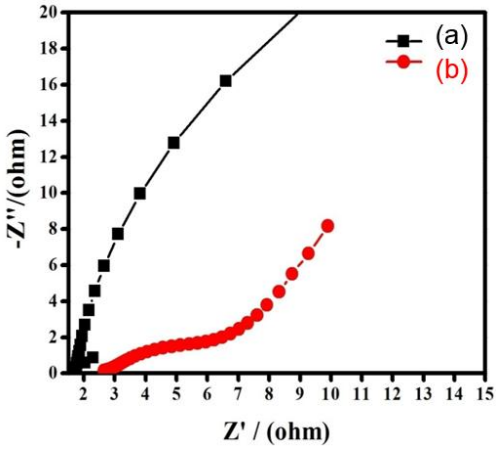

Fig.6. Electrochemical impedance Spectroscopy(EIS) analysis (a) CF and (b) MoS_2 – CF.

Figure 6 represents the electrochemical impedance spectra(EIS) of CF and MoS_2 – CF. Figure 6(a) depicts the impedance spectra of CF. From Figure 6(b), the impedance plot of MoS_2-CF shows a quadrant circle in the higher frequency region and a 45° capacitive slope in the lower frequency region. The higher frequency intercept of the quadrant circle on the real axis of the impedance plot is the combination of the resistance of the electrolyte, the intrinsic resistance of the active material of MoS_2 -CF and the contact resistance between the active material MoS_2 and the current collector CF.

Conclusions

Formation of hierarchical 2D MoS_2 nanostructures over the carbon fabric (CF) was demonstrated using a simple hydrothermal route. FE-SEM analysis exposed the formation of MoS_2 nanospheres like morphology over the CF with homogeneity. FE-SEM results are in good agreement with XRD and Raman results. Electrochemical analysis revealed the excellent electrochemical performance of MoS_2 - CF electrode with the specific capacitance value of 441 F/g at a scan rate of 10mV/s, suggesting that it is a potential electrode material for high power applications.

Conflicts of Interest

The authors declare no conflicts of interest.

Acknowledgments

This work was financially supported in part by a JST CREST Grant Number JPMJCR15Q7, Japan.

References

[1] C. D. Lokhande, D. P. Dubal, and O. S. Joo, Current Appl. Phys., 11, (2011), 255.

[2] G. Wang, L. Zhang, and J. Zhang, Chem. Soc. Rev., 41, (2012), 797.

[3] M. Salanne, B. Rotenberg, K. Naoi, K. Kaneko, P. L. Taberna, C.P. Grey, B. Dunn, and P. Simon, Nat. Energy, 1, (2016) 16070.

[4] Y.A. Kumar, S.S. Rao, D. Punnoose, C.V. Tulasivarma, C.V. Gopi, K. Prabakar, and H. J. Kim, Royal Soc. open sci., 4, (2017) 170427.

[5] J. Zhang, H. Guan, Y. Liu, Y. Zhao, and B. Zhang, Electrochimica Acta, 258, (2017) 182.

[6] Y. Tao, L. Ruiyi, Z. Lin, M. Chenyang, and L. Zaijun, Electrochimica Acta, 176, (2015) 1153.

[7] J. Jiang, Y. Zhang, P. Nie, G. Xu, M. Shi, J. Wang, Y. Wu, R. Fu, H. Dou, and X. Zhang, Adv. Sustainable Sys., 2, (2018), 1700110.

[8] S. A. Han, R. Bhatia and S. W. Kim, Nano Convergence, 2, (2015),17.

[9] J. Huang, D. Hou, Y. Zhou, W. Zhou, G. Li, Z. Tang, L. Li, and S. Chen, J. Mater. Chem. A, 3, (2015), 22886.

[10] F. N. I. Sari, and J. M Ting, Sci. Rep., 7, (2017), 5999.

[11] N. Chen, C. Han, R. Shi, L. Xu, H. Li, Y. Liu, and B. Li, Electrochimica Acta, 283, (2018), 36.

[12] N. Zhang, S. Gan, T. Wu, W. Ma, D. Han, and L. Niu, ACS Appl. Mat. & Inter., 7, (2015), 12193.

[13]. H. Lin, X. Chen, H. Li, M. Yang, and Y. Qi, Mater. Lett., 64, (2010), 1748.

[14] W. Huang, Z. Xu, R. Liu, X. Ye, and Y. Zheng, Mater. Res. Bull., 43, (2008), 2799.

[15] L. Ma, L. M. Xu, X. Y. Xu, Y. L. Luo, and W. X. Chen, Materials Letters, 63, (2009), 2022.

[16]. M. M. Mdleleni, T. Hyeon, and K. S. Suslick, J. Am. Chem. Soc., 120, (1998), 6189.

[17]. Y. W. Lee, G. H. An, S. Lee, J. Hong, B. S. Kim, J. Lee, D. H Kwak, H.J. Ahn, W. Huh, S. N. Cha, K. W. Park, J. I. Sohn, and J. M. Kim, Catalys. Sci. & Tech., 6, (2016), 2085.

[18]. Z. Wang, L. Ma, W. Chen, G. Huang, D. Chen, L. Wang, and J. Y. Lee, RSC Adv., 3, (2013), 21675.

[19]. N. Saha, A. Sarkar, A. B. Ghosh, A. K. Dutta, G. R. Bhadu, P. Paul, and B. Adhikary. RSC Adv., 5, (2015), 88848.

[20]. S. Huang and J. Shi, Ind. Eng. Chem. Res., 53 (2014), 4888.

[21]. Y. B. Yin, J. J. Xu, and Q. C. Liu, Advanced Materials, 28, (2016), 7494.

[22]. M. Govindasamy, S. Shanthi, E. Elaiyappillai, S. F. Wang, P. M. Johnson, H. Ikeda, Y. Hayakawa, S. Ponnusamy, C. Muthamizhchelvan, Electrochimica Acta, 293, (2019), 328.

[23]. G. Plechinger, S. Heydrich, J. Eroms, D. Weiss, C. Schuller, and T. Korn, Appl. Phys. Lett., 101, (2012) 101906.